Contents lists available at ScienceDirect

Journal of Ginseng Research

journal homepage: http://www.ginsengres.org

Research article

Panax ginseng Meyer prevents radiation-induced liver injury via modulation of oxidative stress and apoptosis

CrossMark

Hyeong-Geug Kim [1], Seong-Soon Jang [2], Jin-Seok Lee [1], Hyo-Seon Kim [1], Chang-Gue Son [1],*

[1] Liver and Immunology Research Center, Daejeon Oriental Hospital of Daejeon University, Daehung-ro, Jung-gu, Daejeon, Korea
[2] Department of Radiation Oncology, Daejeon St. Mary's Hospital, The Catholic University of Korea, Daehung-ro, Jung-gu, Daejeon, Korea

A B S T R A C T

Background: Radiotherapy is one of the most important modalities in cancer treatment; however, normal tissue damage is a serious concern. Drug development for the protection or reduction of normal tissue damage is therefore a clinical issue. Herein, we evaluated the protective properties of Panax ginseng Meyer and its corresponding mechanisms.
Methods: C56BL/6 mice were orally pretreated with P. ginseng water extract (PGE; 25 mg/kg, 50 mg/kg, or 100 mg/kg) or intraperitoneally injected melatonin (20 mg/kg) for 4 d consecutively, then exposed to 15-Gy X-ray radiation 1 h after the last administration. After 10 d of irradiation, the biological properties of hematoxicity, fat accumulation, histopathology, oxidative stress, antioxidant activity, pro-inflammatory cytokines, and apoptosis signals were examined in the hepatic tissue.
Results: The irradiation markedly induced myelosuppression as determined by hematological analysis of the peripheral blood. Steatohepatitis was induced by X-ray irradiations, whereas pretreatment with PGE significantly attenuated it. Oxidative stress was drastically increased, whereas antioxidant components were depleted by irradiation. Irradiation also notably increased serum liver enzymes and hepatic protein levels of pro-inflammatory cytokines. Those alterations were markedly normalized by pretreatment with PGE. The degree of irradiation-induced hepatic tissue apoptosis was also attenuated by pretreatment with PGE, which was evidenced by a terminal deoxynucleotidyl transferase 2′-deoxyuridine 5′-triphosphate nick-end labeling assay, western blotting, and gene expressions analysis, particularly of apoptotic molecules.
Conclusion: We suggest that PGE could be applicable for use against radiation-induced liver injury, and its corresponding mechanisms involve the modulation of oxidative stress, inflammatory reactions, and apoptosis.

1. Introduction

Hepatocellular carcinoma (HCC) ranks fifth among the world's most common malignancies and it is also the third most common cause of cancer-related death worldwide [1]. Overall, HCC is newly developed in approximately 1,000,000 patients every year, and 600,000/yr people die of it [2]. The incidence of HCC has rapidly risen due to increasing numbers of patients who are infected with hepatitis C, abuse alcohol, or have nonalcoholic steatohepatitis [3,4]. With regards to the treatment of HCC, various medical modalities, such as the transcatheter hepatic artery chemo embolization and

radiofrequency ablation, have been developed as palliative care methods, providing clinical efficacy and relative convenience for patients, particularly for those with localized HCC [5].

Meanwhile, radiotherapy plays an important role in efficiently treating locally advanced HCC or a metastasized tumor from other organs [6]. Radiotherapy is used in treatment when access to the above modalities is impossible, especially at the late stages of HCC [7]. Moreover, the liver is a common target organ into which other cancers from extrahepatic sites metastasize most frequently; e.g., 10–25% of patients have surgery for primary colorectal cancer due to liver metastasis [8]. Radiotherapy is also one of main medical

modalities used to manage cholangiocarcinoma, another form of liver tumor, especially when it is in an unresectable state [9]. In the above situations, radiation-induced liver injury (RILI) of the normal tissue is a critical factor limiting the application of radiotherapy [10]. It is known that an approximately 5% risk of RILI occurs when radiation is applied to the entire liver tissue in a 30-Gy dose, the minimally effective clinical dose. However, the risk rates rapidly rise more than approximately 50% by 40 Gy. When patients were exposed to 60 Gy of radiation, the most effective dose for killing HCC, approximately 76% of them died of hepatic failure rapidly after the onset of radiation. In addition, liver tissue is the most vulnerable to radiation [11], and has a high chance of being exposed to radiation during radiotherapy for cancers of other sites, especially of the upper abdomen or whole abdomen regions [12].

The high energy from radiation generates free radicals such as hydroxyl radicals and aqueous electrons through the interaction of ionizing radiation with intracellular water molecules, which leads to cellular damage [13]. Some agents show protective effects against the radiotherapy-induced tissue injury in both animal-based experiments and clinical trials. Amifostine (WR-2721) is well known as a free radical scavenger, which protects tissues from radiotherapy-related side effects, especially radio-pneumonitis [14]. However, this agent shows toxicity at the optimal doses of radioprotection, and accompanies a relatively high expense and discomfort of intravenous administration before fractionized radiotherapy [15]. Thus, it is critical issue to develop a radioprotective agent with high efficacy and low toxicity. Therefore, plant-derived phytochemicals or natural products have been adapted as candidates by many investigators.

Panax ginseng Meyer, also called Korean ginseng, has been used as a tonic or herbal medicine for thousands of years, particularly in East Asia. *P. ginseng* shows pharmaceutical effects on various diseases including type II diabetes mellitus, cardiovascular disorders, and chronic fatigue disorders in traditional usages as well as in current clinical studies [16]. *P. ginseng* has also ameliorated the side effects of gastrointestinal troubles and pneumonitis by X-ray irradiation (IR) in animal-based experimental models [17,18]. In terms of safety, *P. ginseng* is verified [19]; therefore, it is now used as a functional food worldwide.

In the present study, we aimed to investigate protective effects of *P. ginseng* against RILI liver injury and its corresponding mechanisms using a mouse model exposed to a high dose of X-ray IR.

2. Materials and methods

2.1. Preparation of P. ginseng extract and fingerprinting analysis

P. ginseng root was obtained from Ginseng Nonghyup (Keumsan, South Korea). Sliced ginseng roots (1.2 kg) were boiled in 6.5 L of water for 100 min at 100°C using a high-speed automatic pressure earthen pot (Kyung-Hee Co-operation, Seoul, South Korea), and the extraction procedure was then repeated with 4.5 L of water. The *P. ginseng* extract (PGE) was then centrifuged for 30 min at 1,500 rpm, and the supernatant was lyophilized using a vacuum-freeze-drying system and stored at −20°C. The extraction yield was 7.1%.

A limulus amebocytelysate assay was performed to determine the endotoxin levels. The amounts of protopanaxadiol and protopanaxatriol ginsenosides in the PGE were estimated using an Alliance HPLC system (Waters, Milford, MA, USA). Three protopanaxadiol ginsenosides (Rb1, Rc, and Rd,) and three protopanaxatriol ginsenosides (Re, Rg1, and Rg2) were used as reference compounds. Standards for ginsenosides Rg3 and Re were purchased from Wako Chemical Co. (Tokyo, Japan) and Santa Cruz Biotechnology Inc. (Dallas, TX, USA), respectively, whereas the

other ginsenosides were purchased from Sigma-Aldrich Co. (St. Louis, MO, USA). For chemical analysis, all standards were of HPLC grade. One gram of PGE and the six ginsenoside mixtures were dissolved in distilled water and subjected to HPLC. For the quantitative analysis of the PGE, each ginsenoside solution was prepared as six serially diluted concentrations.

All of the calibration curves were attained by assessing the peak areas in the range of 0.25−20 mg/L for all of the standard samples. The column was eluted with solvents A (18% acetonitrile) and B (80% acetonitrile) at a flow rate of 2.5 mL/min. The following solutions were used: 100% A and 0% B changed over 32 min, 80% A and 20% B to 80 min, 0% A and 100% B to 100 min, and 100% A and 0% B to 110 min. The detection wavelength was set to 230 nm. Figs. 1A and 1B showed that a total of six different ginsenosides were detected in PGE by HPLC analysis. Regarding the quantitative analysis, ginsenoside contents were shown in the range of 0.15 μg/mg to 3.76 μg/mg. Protopanaxadiol ginsenosides Rb1 and Rg3 were similar and were also the most abundant components (3.76 ± 0.02 μg/mg and 3.75 ± 0.05 μg/mg in PGE, respectively; Fig. 1C). The ginsenosides Re, Rc, Rg2, and Rd were present at the concentrations of 0.95 ± 0.01 μg/mg, 0.79 ± 0.12 μg/mg, 0.44 ± 0.06 μg/mg, 0.15 ± 0.01 μg/mg, respectively.

2.2. Animals and experimental design

A total of 48 heads of specific pathogen-free female C57BL/6N mice (8-wk-old, 19−21 g) were obtained from a commercial animal breeder (Daehanbio-link, Chung-buk, South Korea), and acclimated for l wk before the experiment. All of the animals were housed in an environmentally controlled room at $22 \pm 2°C$ and 60 ± 5% relative humidity under 12/12 h light/dark cycle. All of the mice were freely fed commercial pellets (G-Bio, Gyeong-gi, South Korea) and tap water *ad libitum*. The mice were randomly divided into six groups ($n = 8$ for each group): normal (distilled water without radiation), IR only (distilled water with radiation), PGE treatment groups (25 mg/kg, 50 mg/kg, or 100 mg/kg of PGE with radiation), and the positive control group (20 mg/kg of mealtonin with radiation). The distilled water or PGE was orally administered and melatonin was intraperitoneally injected for 4 consecutive d. All of the mice were anesthetized using a ketamine injection (100 mg/kg, intraperitoneally; Yuhan Pharmacy, Gyeong-gi-do, South Korea) and the upper abdomen including the liver of the mice were exposed to a single X-ray radiation dose of 15 Gy at a dose rate of 3 Gy/min using a linear accelerator (Siemens Medical Solutions, Erlangen, Germany), with shielding for the other parts of the mice. The last drug treatment was administered 1 h before X-ray exposure. All of the mice were sacrificed after 10 d of IR under ether anesthesia conditions. The whole blood was isolated via an abdominal vein, the liver tissue was removed and immediately weighed, and was fixed or stored in 10% neutral buffered formalin, RNAlater (Ambion, Austin, TX, USA), or in a deep freezer (−70°C) for histopathological analysis, mRNA expression analysis, and the determination of biochemical parameters, respectively.

Animal experiments were conducted in accordance with the Guide for the Care and Use of Laboratory Animals published by the United States National Institutes of Health. The protocol was approved by the Institutional Animal Care and Use Committee of Daejeon University (approval number DJUARB: DJUARB-2014-004).

2.3. Analysis of hematology and serum levels of liver enzymes

Peripheral blood was isolated from the abdomen via a 12-h fast vein and then collected from the venous plexus with an EDTA-coated capillary tube. The red blood cells, hemoglobin, white blood cells (WBC), and platelets in each sample were measured by a
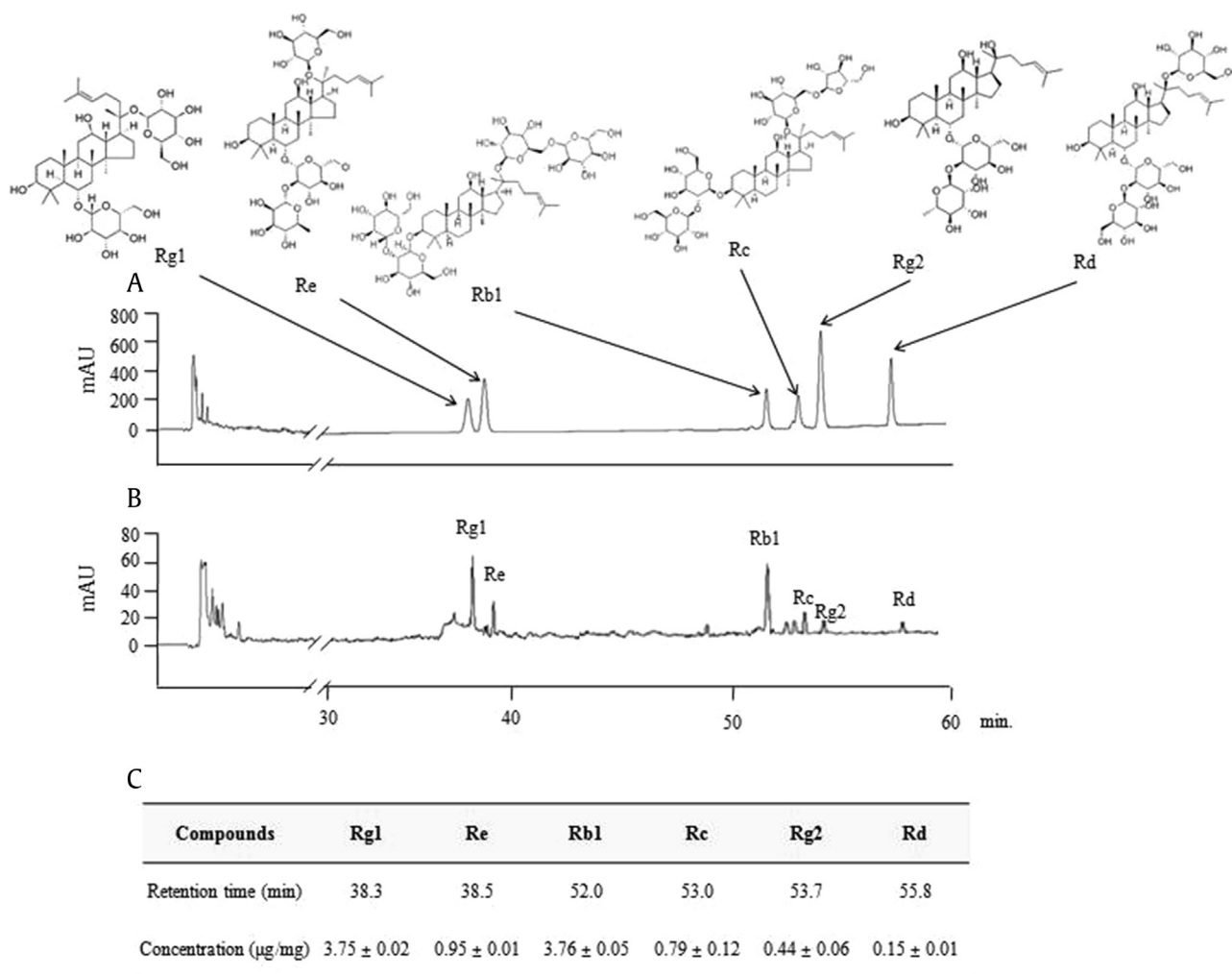
Fig. 1. Fingerprinting analysis of *Panax ginseng extract* (PGE) using HPLC. The PGE and its active compounds were subjected to HPLC. All chromatograms were obtained at a wavelength of 230 nm (details in the text). (A) Histogram of PGE. (B) Standard mixtures. (C) The quantitative analysis of reference compounds in PGE. HPLC, high performance liquid chromatography.

Hemavet 850 automatic analyzer (CDC Technologies, CT, USA). Serum was separated by centrifugation (3,000*g*, 15 min) following blood clotting. The serum levels of aspartatetransaminase (AST), alaninetransaminase (ALT), and alkalinephosphatase (ALP) were determined using an auto chemistry analyzer (Chiron, Emeryville, CA, USA).

2.4. Preparation of hepatic tissue homogenate and determination of protein concentration

For analysis of protein-based parameters, the isolated liver tissues were homogenized in a radioimmunoprecipitation assay buffer and centrifuged at 10,000*g* for 15 min, and protein content was determined using a Bicinchoninic Acid protein assay kit (Sigma, St. Louis, MO, USA). The supernatant was transferred and stored at −70°C until required.

2.5. Histopathological and immunohistochemical examination

The hepatic tissues were fixed in 10% neutral buffered formalin and then embedded in paraffin and cut into 5-μm thick sections for histomorphological and immunohistochemical examination. Hepatic tissue section slides were stained with hematoxylin and eosin (H&E) according to standard procedures. For immunohistochemistry, sections were incubated with 4-hydroxynonenal (4-HNE) primary antibody (1:200; Abcam, Cambridge, UK) and biotinylated secondary antibody (Nichirei Biosciences, Tokyo, Japan), followed by the avidin−biotin−peroxidase complex. The immune-reactive signal was induced by their substrates, 3,3′-diaminobenzidine (Abcam) and 3-amino-9-ethylcarbazole (Abcam). The slides were counterstained with Mayer's hematoxylin and examined under an optical microscope (Leica Microsystems, Wetzlar, Germany).

2.6. Determination of lipid peroxidation in hepatic tissue

Lipid peroxidation levels were evaluated by measuring methylenedioxyamphetamine (MDA) content using the thiobarbituric acid reactive substances method, as described previously [20]. The absorbance of the supernatant was measured at 535 nm and 520 nm, and compared with a standard value (freshly prepared triethyl phosphate solution).

2.7. Determination of total reactive oxygen species in the hepatic tissue

Total reactive oxygen species (ROS) assay was performed using a previous method with slight modifications [21]. The measurement

of total ROS was measured using a microplate reader at 505 nm and 37°C (Molecular Device Corp., Sunnyvale, CA, USA). The ROS 1 unit was equal to 1 μg/mL H_2O_2. Serum nitric oxide levels were determined with the Griess method using Griess' reagent [1% sulfanilamide, 0.1% N-(1-naphthyl) ethylenediamine hydrochloride, and 2.5% H_3PO_4].

2.8. Determination of total antioxidant capacity in hepatic tissue

The total antioxidant capacity (TAC) was determined using a using myoglobin solution with 2,2′-azino-bis [22]. After reacting with the myoglobin/2,2′-azino-bis solution and samples, 2.5mM H_2O_2 was added. The absorbance of TAC was measured at 600 nm using a spectrophotometer 5 min after adding H_2O_2. TAC was expressed as the Trolox equivalents antioxidant capacity.

2.9. Determination of glutathione, glutathione-peroxidase, and glutathione-reductase in hepatic tissue

Total glutathione (GSH) content was determined by 5,5′-dithiobis-(2-nitrobenzoic acid) yielding a yellow chromospheres assay and absorbance at 412 nm was measured using a spectrophotometer [23]. GSH levels were determined from a standard curve using reduced GSH and expressed as μM/mg protein.

The activity of GSH-peroxidase was calculated using a previous method with a slight modification [24] using nicotinamide adenine dinucleotide phosphate (NADPH) reagent [5mM NADPH, 42mM GSH, 10 units/mL GSH reductase (GSH-Rd) in 1.25 mL of distilled water] with tert-butyl hydroperoxide solution which measured at 340 nm using a UV-visible spectrophotometer (Varian, Agilent Technologies, Santa Clara, CA, USA). Enzyme activity was represented according to the following formula: U/mL = (ΔA340 × dilution factor)/(6.22 × sample volume in mL). GSH-Rd activity was determined using 5,5′-dithiobis-(2-nitrobenzoic acid) with NADPH oxidation and reduction power [25].

2.10. Determination of superoxide dismutase and catalase activity in hepatic tissue

Superoxide dismutase (SOD) activity in hepatic tissue was determined using a SOD assay kit (Dojindo Laboratories, Kumamoto, Japan) according to the manufacturer' protocol. Bovine erythrocyte SOD (Sigma) was used a standard. 20 μL of standard or diluted hepatic tissue homogenate were mixed with 200 μL of WST-1 working solution in a 96-well plate. Subsequently, 20 μL of enzyme working solution were added to each well and thoroughly mixed. The plate was incubated at 37°C for 20 min, and was measured at 450 nm using a microplate reader (Molecular Device Corp., Sunnyvale, CA, USA).

Catalase activity in the hepatic tissue was determined according to the previous method [26]. The protein sample reacted with hydrogen and Purpald solution (22.8mM of Purpald in 2N potassium hydroxide). The absorbance at 550 nm of the purple formaldehyde adduct was measured using a spectrophotometer.

2.11. Determination of tumor necrosis factor-α and interleukin-6 levels in hepatic tissue

Hepatic protein levels of tumor necrosis factor-α (TNF-α) and interleukin-6 (IL-6) were measured using commercial enzyme-linked immunosorbent assay kits according to the manufacturers' instructions (Biosource, Camarillo, CA, USA). The absorbance at 450 nm and 570 nm was measured using a spectrophotometer (Molecular Device Corp.).

2.12. Quantification of apoptotic hepatocytes in hepatic tissue

The terminal deoxynucleotidyl transferase 2′-deoxyuridine 5′-triphosphate nick-end labeling assay (TUNEL) assay was performed to detect apoptotic cells in hepatic tissues using a DeadEnd Fluorometric TUNEL System (Promega, Madison, WI, USA). Briefly, hepatic tissues were fixed in 10% formalin and embedded with paraffin. After deparaffinization and washing, the tissue specimens were incubated with proteinase K at room temperature for 10 min. Then, the sections were fixed in phosphate-buffered saline based 4% methanol-free formaldehyde solution. After several washes, the specimens were incubated with terminal deoxynucleotidyl transferase, recombinant enzyme at 37°C for 60 min in the humidified chamber by avoiding direct light. Tissue sections were immersed in the saline-sodium citrate solution for 15 min at room temperature after incubation, and washed several times for completing removals of unincorporated fluorescein-12-2′-deoxyuridine 5′-triphosphate. After that, the apoptotic cells were immediately analyzed under a fluorescence microscope using a standard fluoresce in filter set to view the green fluorescence at 520 ± 20 nm (100× magnification; Olympus, Center Valley, PA, USA). The number of TUNEL-positive cells was counted from five randomly selected fields at 100× magnification per liver sample. Results were expressed as the mean number of TUNEL-positive apoptotic hepatocytes per microscopic field.

2.13. Gene expression analysis by quantitative real-time polymerase chain reaction

Total RNA was extracted from hepatic tissue samples with Trizol reagent (Molecular Research Center, Cincinnati, OH, USA). The cDNA was synthesized from total RNA (2 μg) in a 20-μL reaction using a High-Capacity cDNA reverse transcription kit (Ambion). The primers for Bax, Bcl-2, and Bcl-xL, and β-actin were as follows (forward and reverse) for Bax: AGA CAC CTG AGC TGA CCT TGG A and GAG ACA CTC GCT CAG CTT G; for Bcl-2 GGG ATG CCT TTG TGG AAC TAT ATG and CTG AGC AGG GTC TTC AGA GAC A; for Bcl-xL: ACC GCA GAG CGT TCA GTG AT and CCA TCC CGA AAG AGT TCA TTC A; and for β-actin: CGT GCG TGA CAT CAA AGA GAA and ACC GCT CGT TGC CAA TAG TG, respectively. Results were normalized using β-actin as the reference gene, and are represented as percentages versus the reference gene. Real-time polymerase chain reaction (PCR) reactions were conducted using PikoReal Real-Time PCR System (Thermo Scientific, San Jose, CA, USA) and performed according to the manufacturer's protocol. Reactions were performed in a total volume of 10 μL, containing 1.5 μL of cDNA, 5 μL of SYBR Green qPCR Master Mix (K0259, Thermo Scientific, San Jose, CA, USA), 0.5 μL of each primer, and 3 μL of water (R0581, Thermo Scientific).PCR amplification cycles were carried out as follows: 30 s at 98°C, 40 cycles of 5 s at 98°C, 10 s at 65°C, and 30 s at 72°C. For each sample, two reactions were performed at the same time. One reaction was performed to determine the mRNA level of the target gene, and the second was performed to determine level of β-actin.

2.14. Western blotting analysis

Whole liver homogenates were prepared from liver samples according to the previously described [27]. Protein extracts from the hepatic tissues (40 μg for each) were resolved in the sodium dodecyl sulfate-polyacrylamide gel electrophoresis. After blocking membrane, immunoblotting was performed based on the manufacturer's instruction for each primary antibody against p53, Bax, Bcl-2, and Bcl-xL (all of primary antibodies were purchased from the Thermo Scientific Co.). Membranes were then incubated with the

secondary antibodies against rabbit or mouse (Santa Cruz Biotechnology, Inc., CA, USA). Anti-β-actin antibody (Thermo Scientific Co.) was used as the internal control for equal loading of proteins

2.15. Statistical analysis

All data are expressed as means ± standard deviations. The statistical significance differences between the groups were evaluated by one-way analysis of variance followed by *post-hoc* multiple comparisons with Fisher's Least Significant Difference *t*-test using the IBM SPSS statistics software, version 20.0 (SPSS Inc., Chicago, IL, USA). Differences at $p < 0.05$, $p < 0.01$, or $p < 0.001$ were considered statistically significant.

3. Results

3.1. Effects of PGE on the body weights, liver weights, and hematotoxicity

The final body weight was 20.9 ± 0.2 g in the normal group, whereas the IR-only group was significantly decreased as compared with the normal group (17.0 ± 1.4 g, $p < 0.01$). Pretreatment with PGE slightly recovered body weight loss without significance (Table 1). Both the absolute and relative liver mass was significantly reduced by IR and pretreatment with PGE did not affect them (Table 1).

IR drastically decreased the hemoglobin concentration, and number of red blood cells, WBCs (most drastically), and platelets in peripheral blood of mice. The pretreatment with PGE showed a slight protective pattern especially on WBC counts, without statistical significance ($p = 0.07$ for 100 mg/kg). The PGE significantly decreased platelet counts ($p < 0.05$ for 25 mg/kg and 50 mg/kg), in a dose-reverse manner. Melatonin significantly increased platelet counts, but other parameters were not affected (Table 1).

3.2. Effects of PGE on the histopathological analysis

IR caused a steatotic alteration evidenced by measuring H&E staining, whereas pretreatment with PGE remarkably attenuated

these histopathological alterations (Fig. 2A). The 4-HNE signal, which is a potent marker of lipid peroxidation, was strongly enhanced in the IR-only group, but PGE groups showed the reduction of 4-HNE signals (part of the dark brown color in Fig. 2B). Those changes were also attenuated by pretreatment with melatonin.

3.3. Effects of PGE on the IR-induced total ROS level, MDA content, and triglyceride levels in hepatic tissue

Total ROS level was significantly higher by approximately 1.3-fold than that of the normal group, which is significantly attenuated by pretreatment with PGE (especially 100 mg/kg; Fig. 2C). The hepatic MDA contents in the IR-only group was significantly increased by 2.4-fold compared with the normal group, while pretreatment with PGE significantly ameliorated MDA levels as compared with the IR-only group ($p < 0.01$ for 50 mg/kg and 100 mg/kg; Fig. 2D). Hepatic triglyceride levels were also markedly increased by about 1.3-fold in the IR-only group compared with the normal group, whereas PGE pretreatment significantly attenuated it ($p < 0.05$ for 50 mg/kg and $p < 0.01$ for 100 mg/kg, respectively; Fig. 2E).

The melatonin showed similar effects on the hepatic MDA and triglyceride levels, but not total ROS levels.

3.4. Effects of PGE on the IR-induced nonenzymatic antioxidant component alterations in hepatic tissue levels

IR significantly decreased hepatic tissue levels of TAC by approximately 0.8-fold as compared with the normal group, while pretreatment with PGE significantly increased it compared with the control group ($p < 0.05$ for 25 mg/kg, 50 mg/kg, and 100 mg/kg, respectively; Table 1). The total GSH contents in the IR-only group were considerably depleted by 0.5-fold as compared with the normal group, whereas pretreatment with PGE significantly blocked the deterioration as compared with the IR-only group ($p < 0.05$ for 100 mg/kg and $p < 0.01$ for 50 mg/kg, respectively; Table 1).

Pretreatment with melatonin also positively affected TAC and total GSH contents in hepatic tissue.

Table 1
Effects on body and liver weights, as well as antioxidant components

Groups	Normal	IR only	IR with PGE treatment (mg/kg)			IR with Mel 20 (mg/kg)
			25	50	100	
Final body weight (g)	20.9 ± 0.2	17.0 ± 1.4**	17.7 ± 2.6	18.0 ± 1.7	18.0 ± 1.1	16.0 ± 2.0
Absolute liver mass (g)	1.0 ± 0.1	1.2 ± 0.1*	1.1 ± 0.2	1.2 ± 0.1	1.3 ± 0.1	1.0 ± 0.2
Relative liver mass (%)	4.8 ± 0.4	6.8 ± 0.5***	6.5 ± 0.1	6.8 ± 0.1	6.9 ± 0.1	6.7 ± 0.1
RBC (10^6/μL)	9.1 ± 0.2	7.1 ± 0.5**	7.0 ± 0.4	7.4 ± 0.8	7.9 ± 0.5	7.8 ± 0.7
Hemoglobin (g/dL)	15.5 ± 0.3	10.9 ± 0.8***	11.0 ± 0.7	10.1 ± 0.4	9.1 ± 0.6	9.5 ± 1.3
WBC (k/uL)	5.7 ± 1.8	2.0 ± 0.3***	1.7 ± 0.4	2.6 ± 0.3	3.5 ± 1.2	3.3 ± 0.9
Platelet counts (k/uL)	1298.0 ± 221.2	1158.0 ± 57.3	880.2 ± 143.8****	1088.4 ± 43.9****	1012.4 ± 54.2	1368.0 ± 174.2****
Total antioxidant capacity (uM/mg protein)	125.7 ± 13.6	106.1 ± 12.9*	193.5 ± 42.8****	170.3 ± 13.5******	173.9 ± 26.8******	187.1 ± 38.4*****
Total GSH contents (μM/mg protein)	169.3 ± 71.3	85.2 ± 26.2**	152.3 ± 26.2	138.9 ± 23.3*****	112.2 ± 19.9****	110.0 ± 18.5*
GSH-peroxidase activity (units/mg protein)	1.5 ± 2.1	0.7 ± 0.7	0.8 ± 0.5	0.6 ± 0.4	0.8 ± 0.8	0.5 ± 0.2
GSH-reductase activity (units/mg protein)	25.1 ± 2.7	21.2 ± 2.6*	38.7 ± 8.6****	34.1 ± 2.7******	34.7 ± 5.4******	37.4 ± 7.7*****
Catalase activity (units/mg protein)	666.4 ± 134.5	422.6 ± 53.8**	807.7 ± 130.1*****	647.3 ± 196.3****	671.4 ± 162.7****	604.8 ± 411.0
SOD activity (units/mg protein)	23.9 ± 6.5	7.8 ± 1.2***	5.6 ± 2.3	11.6 ± 3.6****	11.5 ± 3.6****	18.3 ± 20.9

Data are expressed as the mean ± standard deviation ($n = 4-7$)
*$p < 0.05$ was compared with the normal group
**$p < 0.01$ was compared with the normal group
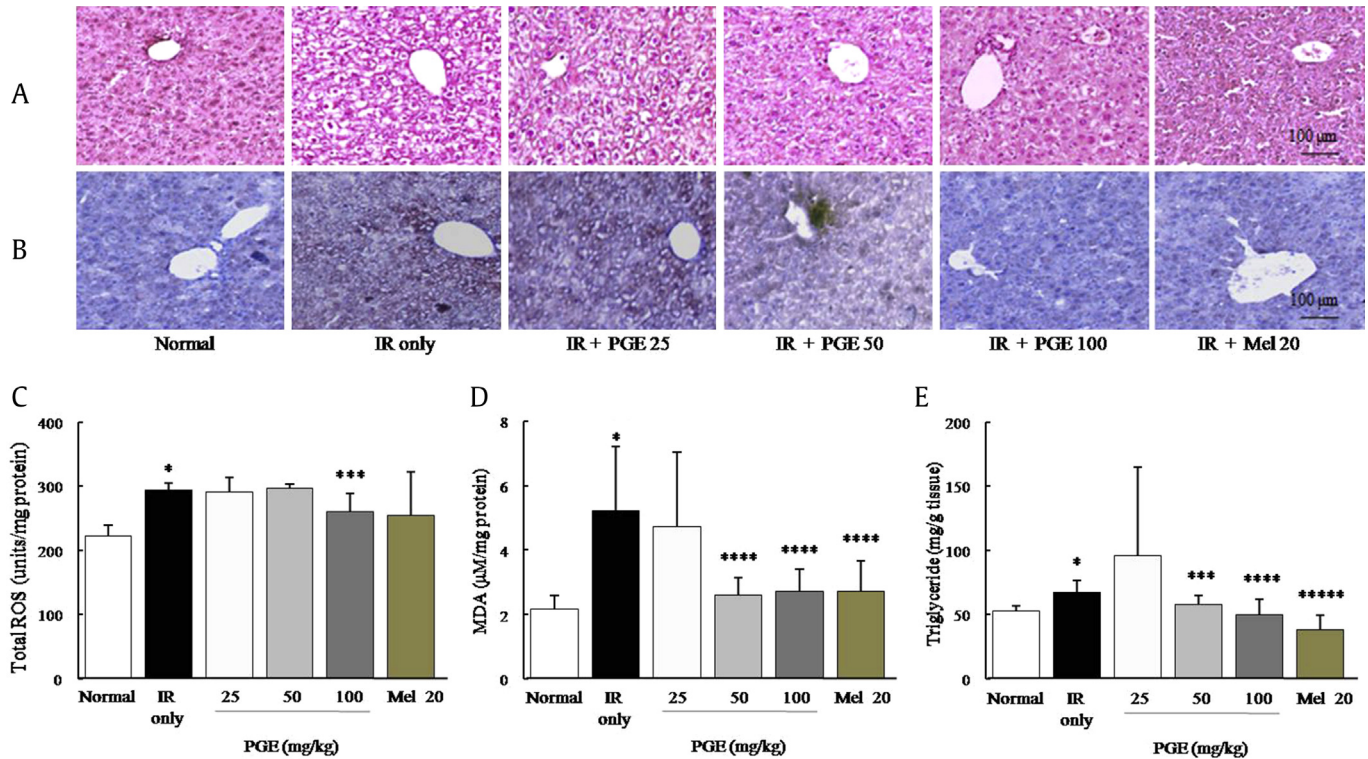***$p < 0.001$ was compared with the normal group
****$p < 0.05$ was compared with the IR-only group
*****$p < 0.01$ was compared with the IR-only group
******$p < 0.001$ was compared with the IR-only group
GSH, glutathione; IR, irradiation; Mel, melatonin; PGE, *Panax ginseng* extract; RBC, red blood cells; SOD, superoxide dismutase; WBC, white blood cells

Fig. 2. Histopathological findings and total reactive oxygeb species (ROS), malondialdehyde (MDA), and triglyceride (TG) contents in hepatic tissues. (A) The representative photomicrographs of liver sections processed for hematoxylin and eosin staining was examined under the microscopy (100×). (B) The representative photomicrographs of liver sections processed for immunohistochemical staining for 4-hydroxynonenal was examined under the microscopy (100×). Hepatic tissue levels of total (C) ROS, (D) MDA, and (E) TG were determined in hepatic tissue. Data were expressed as the mean ± standard deviation ($n = 8$). *$p < 0.01$ was compared with the normal group. **$p < 0.001$ was compared with the normal group. ***$p < 0.05$ was compared with the IR-only group. ****$p < 0.01$ was compared with the IR-only group. *****$p < 0.001$ was compared with the IR-only group. IR, irradiation; Mel, melatonin.

3.5. Effect of PGE on the IR-induced enzymatic antioxidant components alterations in hepatic tissue levels

15-Gy X-ray IR considerably depleted GSH-Rd, SOD, and catalase activities in hepatic tissues compared with the normal group by approximately 0.8-, 0.3-, and 0.6-fold respectively, whereas pretreatment significantly prevented those deteriorations (GSH-Rd: $p < 0.05$ for 25 mg/kg, $p < 0.001$ for 50 mg/kg and 100 mg/kg; SOD: $p < 0.05$ for 50 mg/kg and 100 mg/kg; catalase: $p < 0.05$ for 50 mg/kg and 100 mg/kg, $p < 0.01$ for 25 mg/kg, respectively; Table 1). The GSH-peroxidase activity was lowered by 0.5-fold in the normal group, and the pretreatment with PGE slightly increased it without significance (Table 1).

Melatonin showed a significant increase of GSH-Rd activities, but not in the others in hepatic tissue.

3.6. Effect of PGE on the IR-induced serum levels of liver enzymes and hepatic protein levels of pro-inflammatory cytokines

15-Gy X-ray IR markedly increased serum levels of AST, ALT, and ALP by approximately 3.2-, 2.1-, and 1.5-fold as compared with the normal group, respectively. Pretreatment with PGE (especially 100 mg/kg) significantly decreased serum levels of ALT and ALP as compared with the IR-only group, but not AST levels ($p < 0.05$ in ALT and ALP, respectively; Fig. 3A).

Protein levels of pro-inflammatory cytokines, such as TNF-α and IL-6, were increased by 2.4- and 1.2-fold in the IR group compared with the normal group, but PGE significantly

ameliorated these elevations ($p < 0.05$ for 50 mg/kg and 100 mg/kg in TNF-α and 25 mg/kg, 50 mg/kg, and 100 mg/kg in IL-6, respectively; Figs. 3A and 3C).

Melatonin showed a similar effect on the serum levels of ALT and ALP, but not pro-inflammatory cytokines in hepatic tissue.

3.7. Effect of PGE on the IR-induced apoptosis signals in hepatic tissue levels

Irradiation notably enhanced the apoptosis cells (stained in nuclei parts as a green fluorescence) by measuring TUNEL staining in the hepatic tissue, while pretreatment with PGE groups considerably reduced them compared with the IR-only group (Figs. 4A and 4B). In the western blot analysis, the pro-apoptotic proteins such as p53 and Bax were markedly increased, whereas antiapoptotic proteins including BcL-2 and BcL-xL were notably decreased by X-ray IR as compared with the normal groups. The above alterations were significantly normalized by pretreatment with PGE (Figs. 5A and 5B).The hepatic gene expression level of *Bax* was approximately 2.1-fold higher, whereas *Bcl-2* and *Bcl-xL* were about 0.7- and 0.8-fold lower than that of the normal group by IR, respectively. Pretreatment with PGE significantly normalized above abnormalities as compared with IR-only group ($p < 0.05$ for 100 mg/kg in *Bcl-2* and *Bcl-xL*, $p < 0.01$ for 50 mg/kg in *Bcl-xL*, and 100 mg/kg in *Bax*, respectively; Fig. 5C).

Pretreatment with melatonin also notably improved the deteriorations of apoptosis signals in the hepatic tissue (Figs. 5A–5C).
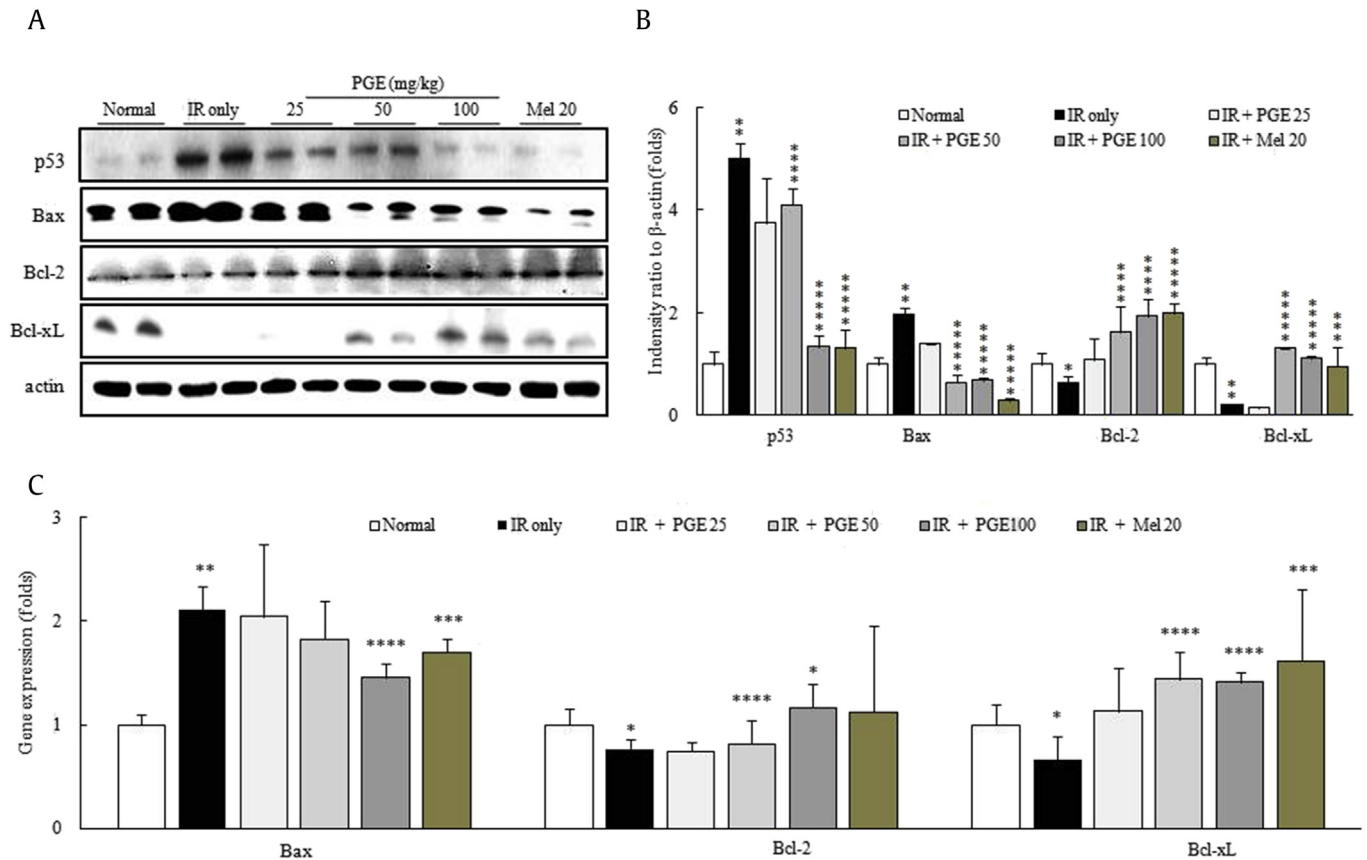
A

B

C
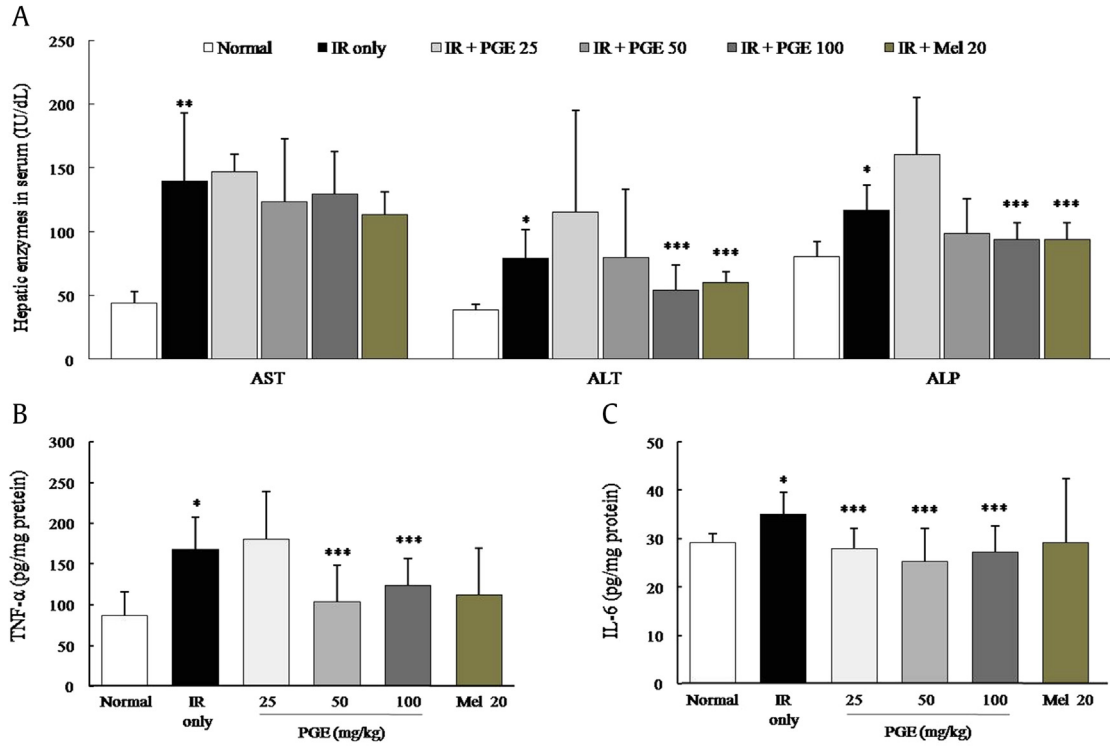
Fig. 3. Serum biochemistries and pro-inflammatory cytokines in hepatic tissues. (A) Serum biochemistries including aspartatetransaminase (AST), alaninetransaminase (ALT), and alkalinephosphatase (ALP) were analyzed. (B) Hepatic tissue levels of tumor necrosis factor-α (TNF-α) and (C) interleukin-6 (IL-6) were determined using a commercial enzyme-linked immunosorbent assay kit. Data were expressed as the mean ± standard deviation ($n = 8$). *$p < 0.01$ was compared with the normal group. **$p < 0.001$ was compared with the normal group. ***$p < 0.05$ was compared with the IR-only group. ****$p < 0.01$ was compared with the IR-only group. *****$p < 0.001$ was compared with the IR-only group. IR, irradiation; Mel, melatonin; PGE, *Panax ginseng* extract.

4. Discussion

We investigated the PGE's effects on RILI and its potential corresponding mechanisms. To produce the RILI mice model, we exposed mice to an X-ray at a single dose of 15 Gy, approximately equivalent to 60 Gy for humans, which is a 2-fold higher dose than that for clinical use, resulting in 5–50% higher probabilities for liver failure within 5 yr [28]. Although we irradiated whole liver in a localized manner, IR-induced hematoxicity, including severe leucopenia and weight loss occurred besides liver injury (Table 1; Figs. 3A, 2A). PGE pretreatment significantly protected the hepatic injury, as evidenced by normalization of ALT and ALP, but not AST (Fig. 3A). Some portions of AST might be released from not only liver but also heart or muscles, because it is known to be distributed in heart and muscle, unlike ALT and ALP [29]. Additionally, IR markedly induced hepatic steatosis, as supported by histological findings and the increase of hepatic triglyceride levels; then, it was significantly ameliorated by PGE pretreatment (Figs. 2A and 2E). The steatotic alteration is a representative pathological feature of RILI [30]. The radiation-induced thrombocytopenia was augmented

A

B
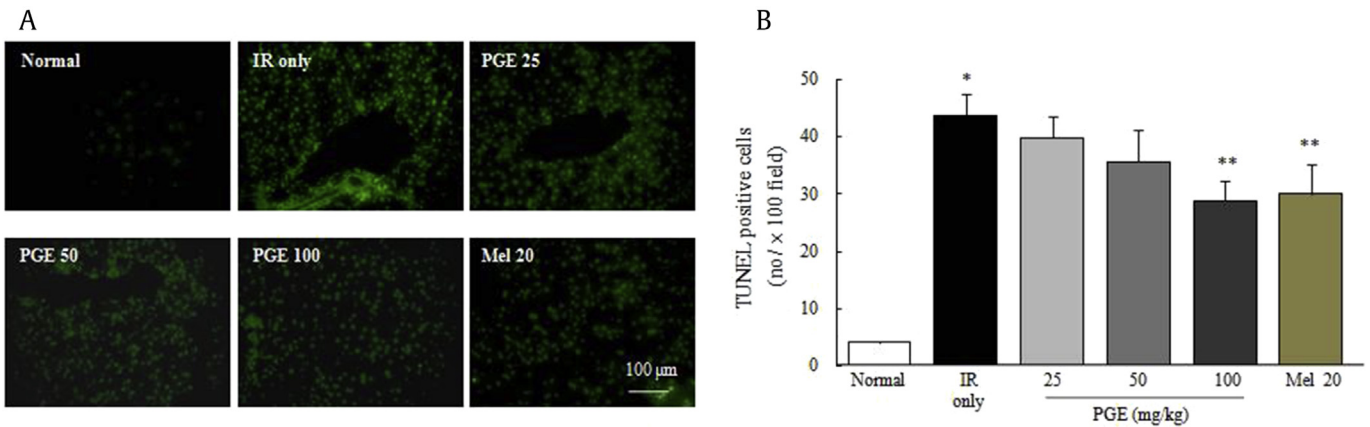
Fig. 4. Terminal deoxynucleotidyl transferase 2′-deoxyuridine 5′-triphosphate nick-end labeling assay (TUNEL) assay in hepatic tissue. (A) Apoptotic hepatocytes in hepatic tissue were identified by TUNEL assay and (B) the TUNEL-positive cells in hepatic tissues were quantified (100×). Data were expressed as the mean ± standard deviation ($n = 8$). *$p < 0.01$ compared with the normal group. **$p < 0.01$ compared with the IR-only group. IR, irradiation; Mel, melatonin; PGE, *Panax ginseng* extract.

occupying cancers [42]. Only one-third of patients with HCC or cholangiocarcinoma can possibly be treated with curative therapies. Moreover, the prevalence of the above cancers has been increasing every year, thus it is estimated that the demand for radiotherapy will be increased [7]. To date, no therapeutic agent to prevent or reduce RILI exists. *P. ginseng* has been commonly used to treat a wide variety of diseases [43]. Previous studies reported that *P. ginseng* beneficially affected side effects or adverse effects during the IRs [44,45]; however, no study has been conducted regarding RILI.

In the current study, we found the protective effects of PGE against RILI primarily through antioxidant actions and modulation of apoptosis signals. There are a number of studies on antioxidant effects of *P. ginseng* in chemotherapy and IR animal models [46–48]. Previous studies showed that the ginsenosides Rg1 and Rb1, major components of *P. ginseng*, ameliorated the apoptosis signals via modulation of the p53 protein in HaCaT cells under UV-IR conditions [49]. In addition, the ginsenoside Rg1 also ameliorated caspase-3 activity in an isoflurane-induced apoptotic rat model [50]. Quantitative analysis of PGE revealed that Rg1 and Rb1 are most abundant compounds in PGE (Fig. 1), and thus Rg1 and Rb1 would be thought of as active compounds in our experimental model. However, our previous study indicated that nonginsenoside fractions of *P. ginseng* also exerted protective effects, comparable with the ginsenoside fraction, on cisplatin-induced gastric damage in a rat model [51], and others also showed similar effects using nonsaponin fractions [52]. Moreover, the general formula of *P. ginseng* traditionally comprises the whole fraction, as the PGE used in our current study. From our data, 50 mg/kg and 100 mg/kg of PGE showed consistently positive effects, but 25 mg/kg of PGE did not. This means that the different effects occur in a dose-dependent manner, which must be considered in clinical studies or use.

The current study model has a limitation, which is dissimilar to clinical studies irradiating bodies under-containing tumor masses. Other studies have proven that *P. ginseng* or its derived compounds show dominant effects on the various cancers using *in-vivo* models [53,54]. Additionally, one study found that IR and *P. ginseng* also synergistically recovered the survival rate of liver cancer [55]. Thus our data provided the experimental evidence for the clinical relevance of *P. ginseng* as a potential herbal remedy.

Taken together, we proved the protective effects of *P. ginseng* on RILI through amelioration of oxidative stress as well as modulation of apoptosis signals. Our results indicate that *P. ginseng* could be applied for preventing RILI in radiation therapy.

Conflicts of interest

All contributing authors declare no conflicts of interest.

Acknowledgments

References

[1] Ferlay J, Soerjomataram I, Dikshit R, Eser S, Mathers C, Rebelo M, Parkin DM, Forman D, Bray F. Cancer incidence and mortality worldwide: sources, methods and major patterns in GLOBOCAN 2012. Int J Cancer 2015;136:E359–86.
[2] Gomaa AI, Khan SA, Toledano MB, Waked I, Taylor-Robinson SD. Hepatocellular carcinoma: epidemiology, risk factors and pathogenesis. World J Gastroenterol 2008;14:4300–8.
[3] Ferro A, Peleteiro B, Malvezzi M, Bosetti C, Bertuccio P, Levi F, Negri E, La Vecchia C, Lunet N. Worldwide trends in gastric cancer mortality (1980–2011), with predictions to 2015, and incidence by subtype. Eur J Cancer 2014;50:1330–44.
[4] Kim JL, Cho KH, Park EC, Cho WH. A single measure of cancer burden combiningincidence with mortality rates for worldwide application. Asian Pac J Cancer Prev 2014;15:433–9.
[5] Delanian S, Lefaix JL. Current management for late normal tissue injury: radiation-induced fibrosis and necrosis. Semin Radiat Oncol 2007;17:99–107.
[6] Zhou ZH, Liu LM, Chen WW, Men ZQ, Lin JH, Chen Z, Zhang XJ, Jiang GL. Combined therapy of transcatheter arterial chemoembolization and three-dimensional conformal radiotherapy for hepatocellular carcinoma. Br J Radiol 2007;80:194–201.
[7] Kalogeridi MA, Zygogianni A, Kyrgias G, Kouvaris J, Chatziioannou S, Kelekis N, Kouloulias V. Role of radiotherapy in the management of hepatocellular carcinoma: A systematic review. World J Hepatol 2015;7:101–12.
[8] Nosher JL, Ahmed I, Patel AN, Gendel V, Murillo PG, Moss R, Jabbour SK. Nonoperative therapies for colorectal liver metastases. J Gastrointest Oncol 2015;6:224–40.
[9] Bowling TE, Galbraith SM, Hatfield AR, Solano J, Spittle MF. A retrospectivecomparison of endoscopic stenting alone with stenting and radiotherapy in nonresectablecholangiocarcinoma. Gut 1996;39:852–5.
[10] Ben-Josef E, Normolle D, Ensminger WD, Walker S, Tatro D, Ten Haken RK, Knol J, Dawson LA, Pan C, Lawrence TS. Phase II trial of high-dose conformal radiation therapy with concurrent hepatic artery floxuridine for unresectable intrahepatic malignancies. J Clin Oncol 2005;23:8739–47.
[11] Emami B, Lyman J, Brown A, Coia L, Goitein M, Munzenrider JE, Shank B, Solin LJ, Wesson M. Tolerance of normal tissue to therapeutic irradiation. Int J Radiat Oncol Biol Phys 1991;21:109–22.
[12] Alati T, Van Cleeff M, Strom SC, Jirtle RL. Radiation sensitivity of adult human parenchymal hepatocytes. Radiat Res 1988;115:152–60.
[13] Kim JH, Jenrow KA, Brown SL. Mechanisms of radiation-induced normal tissue toxicity and implications for future clinical trials. Radiat Oncol J 2014;32:103–15.
[14] Mehta V. Radiation pneumonitis and pulmonary fibrosis in nonsmall-cell lung cancer: pulmonary function, prediction, and prevention. Int J Radiat Oncol Biol Phys 2005;63:5–24.
[15] Westbury CB, Yarnold JR. Radiation fibrosis–current clinical and therapeutic perspectives. Clin Oncol (R Coll Radiol) 2012;24:657–72.
[16] Choi J, Kim TH, Choi TY, Lee MS. Ginseng for health care: a systematic review of randomized controlled trials in Korean literature. PLoS One 2013;8:e59978.
[17] Balaji Raghavendran HR, Rekha S, Cho HK, Jang SS, Son CG. Ginsenoside rich fraction of *Panax ginseng* Meyer improve feeding behavior following radiation-induced pica in rats. Fitoterapia 2012;83:1144–50.
[18] Jang SS, Kim HG, Han JM, Lee JS, Choi MK, Huh GJ, Son CG. Modulation of radiation-induced alterations in oxidative stress and cytokine expression in lung tissue by *Panax ginseng* extract. Phytother Res 2015;29:201–9.
[19] Lee NH, Yoo SR, Kim HG, Cho JH, Son CG. Safety and tolerability of *Panax ginseng* root extract: a randomized, placebo-controlled, clinical trial in healthy Korean volunteers. J Altern Complement Med 2012;18:1061–9.
[20] Mihara M, Uchiyama M. Determination of malonaldehyde precursor in tissues by thiobarbituric acid test. Anal Biochem 1978;86:271–8.
[21] Hayashi I, Morishita Y, Imai K, Nakamura M, Nakachi K, Hayashi T. High-throughput spectrophotometric assay of reactive oxygen species in serum. Mutat Res 2007;631:55–61.
[22] Kambayashi Y, Binh NT, Asakura HW, Hibino Y, Hitomi Y, Nakamura H, Ogino K. Efficient assay for total antioxidant capacity in human plasma using a 96-well microplate. J Clin Biochem Nutr 2009;44(1):46–51.
[23] Evans JC, Ellman GL. The ionization of cysteine. Biochim Biophys Acta 1959;33:574–6.
[24] Ursini F, Maiorino M, Brigelius-Flohé R, Aumann KD, Roveri A, Schomburg D, Flohé L. Diversity of glutathione peroxidases. Methods Enzymol 1995;252:38–53.
[25] Smith IK, Vierheller TL, Thorne CA. Assay of glutathione reductase in crude tissue homogenates using 5,5′-dithiobis(2-nitrobenzoic acid). Anal Biochem 1988;175:408–13.
[26] Wheeler CR, Salzman JA, Elsayed NM, Omaye ST, Korte Jr DW. Automated assays for superoxide dismutase, catalase, glutathione peroxidase, and glutathione reductase activity. Anal Biochem 1990;184:193–9.
[27] Chung J, Chavez PR, Russell RM, Wang XD. Retinoic acid inhibits hepatic Jun N-terminal kinase-dependent signaling pathway in ethanol-fed rats. Oncogene 2002;21:1539–47.
[28] Milano MT, Constine LS, Okunieff P. Normal tissue tolerance dose metrics for radiation therapy of major organs. Semin Radiat Oncol 2007;17:131–40.
[29] Josef O, Marcia R, Martin S, Wendy B, Shelli S. The current state of serum biomarkers of hepatotoxicity. Toxicology 2008;245:164–205.
[30] Guha C, Sharma A, Gupta S, Alfieri A, Gorla GR, Gagandeep S, Sokhi R, Roy-Chowdhury N, Tanaka KE, Vikram B, et al. Amelioration of radiation-induced liver damage in partially hepatectomized rats by hepatocyte transplantation. Cancer Res 1999;59:5871–4.
[31] Robbins ME, Zhao W. Chronic oxidative stress and radiation-induced late normal tissue injury: a review. Int J Radiat Biol 2004;80:251–9.
[32] Spitz DR, Azzam EI, Li JJ, Gius D. Metabolic oxidation/reduction reactions and cellular responses to ionizing radiation: a unifying concept in stress response biology. Cancer Metastasis Rev 2004;23:311–22.
[33] Sies H. Oxidative stress: a concept in redox biology and medicine. Redox Biol 2015;4:180–3.

[34] Bryan N, Ahswin H, Smart N, Bayon Y, Wohlert S, Hunt JA. Reactive oxygen species (ROS)—a family of fate deciding molecules pivotal in constructive inflammation and wound healing. Eur Cell Mater 2012;24: 249—65.

[35] Malik IA, Moriconi F, Sheikh N, Naz N, Khan S, Dudas J, Mansuroglu T, Hess CF, Rave-Fränk M, Christiansen H, et al. Single-dose gamma-irradiation induces up-regulation of chemokine gene expression and recruitment of granulocytes into the portal area but not into other regions of rat hepatic tissue. Am J Pathol 2010;176:1801—15.

[36] Rodemann HP, Blaese MA. Responses of normal cells to ionizing radiation. Semin Radiat Oncol 2007;17:81—8.

[37] Morita A, Ariyasu S, Wang B, Asanuma T, Onoda T, Sawa A, Tanaka K, Takahashi I, Togami S, Nenoi M, et al. AS-2, a novel inhibitor of p53-dependent apoptosis, prevents apoptotic mitochondrial dysfunction in a transcription-independent manner and protects mice from a lethal dose of ionizing radiation. Biochem Biophys Res Commun 2014;450:1498—504.

[38] Saha S, Woodbine L, Haines J, Coster M, Ricket N, Barazzuol L, Ainsbury E, Sienkiewicz Z, Jeggo P. Increased apoptosis and DNA double-strand breaks in the embryonic mouse brain in response to very low-dose X-rays but not 50 Hz magnetic fields. J R Soc Interface 2014;11(100):20140783. 1—10.

[39] Epperly MW, Epstein CJ, Travis EL, Greenberger JS. Decreased pulmonary radiation resistance of manganese superoxide dismutase (MnSOD)-deficient mice is corrected by human manganese superoxide dismutase-Plasmid/Liposome (SOD2-PL) intratracheal gene therapy. Radiat Res 2000;154:365—74.

[40] Coleman MC, Olivier AK, Jacobus JA, Mapuskar KA, Mao G, Martin SM, Riley DP, Gius D, Spitz DR. Superoxide mediates acute liver injury in irradiated mice lacking sirtuin 3. Antioxid Redox Signal 2014;20:1423—35.

[41] Feng M, Ben-Josef E. Radiation therapy for hepatocellular carcinoma. Semin Radiat Oncol 2011;21:271—7.

[42] Lawrence TS, Robertson JM, Anscher MS, Jirtle RL, Ensminger WD, Fajardo LF. Hepatic toxicity resulting from cancer treatment. Int J Radiat Oncol Biol Phys 1995;31:1237—48.

[43] Xiang YZ, Shang HC, Gao XM, Zhang BL. A comparison of the ancient use of ginseng in traditional Chinese medicine with modern pharmacological experiments and clinical trials. Phytother Res 2008;22:851—8.

[44] Lee TK, Johnke RM, Allison RR, O'Brien KF, Dobbs Jr LJ. Radioprotective potential of ginseng. Mutagenesis 2005;20:237—43.

[45] Verma P, Jahan S, Kim TH, Goyal PK. Management of radiation injuries by Panax ginseng extract. J Ginseng Res 2011;35:261—71.

[46] Kim SR, Jo SK, Kim SH. Modification of radiation response in mice by ginsenosides, active components of Panax ginseng. In Vivo 2003;17:77—81.

[47] Kumar M, Sharma MK, Saxena PS, Kumar A. Radioprotective effect of Panax ginseng on the phosphatases and lipid peroxidation level in testes of Swiss albino mice. Biol Pharm Bull 2003;26:308—12.

[48] Wei X, Su F, Su X, Hu T, Hu S. Stereospecific antioxidant effects of ginsenoside Rg3 on oxidative stress induced by cyclophosphamide in mice. Fitoterapia 2012;83:636—42.

[49] Wang XY, Wang YG, Wang YF. Ginsenoside Rb1, Rg1, and three extracts of traditional Chinese medicine attenuate ultraviolet B-induced G1 growth arrest in HaCaT cells and dermal fibroblasts involve down-regulating the expression of p16, p21, and p53. Photodermatol Photoimmunol Photomed 2011;27:203—12.

[50] Miao HH, Zhen Y, Ding GN, Hong FX, Xie ZC, Tian M. Ginsenoside Rg1 attenuates isoflurane-induced caspase-3 activation via inhibiting mitochondrial dysfunction. Biomed Environ Sci 2015;28:116—26.

[51] Sathyanath R, Hanumantha Rao BR, Kim HG, Cho JH, Son CG. Saponin and non-saponin fractions of red ginseng ameliorate cisplatin-induced pica in rats. Pharm Biol 2013;51:1052—60.

[52] Min KT, Koo BN, Kang JW, Bai SJ, Ko SR, Cho ZH. Effect of ginseng saponins on the recombinant serotonin type 3A receptor expressed in xenopus oocytes: implication of possible application as an antiemetic. J Altern Complement Med 2003;9:505—10.

[53] Kim HS, Lim JM, Kim JY, Kim Y, Park S, Sohn J. Panaxydol, a component of Panax ginseng, induces apoptosis in cancer cells through EGFR activation and ER stress and inhibits tumor growth in mouse models. Int J Cancer 2016;138: 1432—41.

[54] Nishino H, Tokuda H, Ii T, Takemura M, Kuchide M, Kanazawa M, Mou XY, Bu P, Takayasu J, Onozuka M, et al. Cancer chemoprevention by ginseng in mouse liver and other organs. J Korean Med Sci 2001;16:S66—9.

[55] You JS, Hua DM, Chen KT, Huang HF. Combined effects of ginseng and radiotherapy on experimental liver cancer. Phytother Res 1995;9:331—5.